Title
Aerodynamic Forces on Truck Models, Including Two Trucks in Tandem

Authors
Hammache, Mustapha
Michaelian, Mark
Browand, Fred

Publication Date
2001-10-01

CALIFORNIA PATH PROGRAM
INSTITUTE OF TRANSPORTATION STUDIES
UNIVERSITY OF CALIFORNIA, BERKELEY

Aerodynamic Forces on Truck Models, Including Two Trucks in Tandem

Mustapha Hammache, Mark Michaelian, Fred Browand
University of Southern California

California PATH Research Report
UCB-ITS-PRR-2001-27

This work was performed as part of the California PATH Program of the University of California, in cooperation with the State of California Business, Transportation, and Housing Agency, Department of Transportation; and the United States Department of Transportation, Federal Highway Administration.

Report for MOU 387, TO 4214

October 2001

ISSN 1055-1425

Aerodynamic Forces on Truck Models, Including Two Trucks in Tandem

by
Mustapha Hammache, Mark Michaelian and Fred Browand
Aerospace and Mechanical Engineering Department
University of Southern California

Executive Summary

The present wind tunnel experiment describes 6-component force and moment data measured for both the cab and the trailer of a simplified model truck. Forces and moments are presented in *coefficient* form. The cab is sufficiently smooth that no flow separation occurs at zero yaw. The trailer has rounded forward vertical edges and sharp upper and lower edges. Both cab and trailer have wheels. The test matrix includes variation of the cab-trailer gap, and the yaw angle between the model plane of symmetry and the axis of the wind tunnel. The yaw angle is meant to account for the presence of an over-the-road side-wind. Cab-trailer gap separation is varied from 0-1.55$\sqrt{A}$, where A is the frontal cross-sectional area of the trailer. Yaw angle is varied from 0-16 degrees.

At small gap and zero yaw, the trailer drag coefficient is of the order of (0.15)—a factor of three smaller than the cab drag coefficient. Trailer drag coefficient increases to about (0.45) as the gap increases to 1.55$\sqrt{A}$. The increase is not linear with separation. Cab drag coefficients are of the order of (0.45) for this model, but can be 30% greater at certain critical gap spacings between 0.25$\sqrt{A}$ and .50$\sqrt{A}$. The side forces on cab and trailer depend primarily on yaw angle—both side force coefficients exceed unity at a yaw angle of 16 degrees. Rolling moment measurements show the line of action of the side force lies just below the horizontal mid-plane of the cab (or trailer).

A second experiment provides drag information for two trucks in tandem with a variable spacing between the trucks. In this case the cab and trailer remain fixed at zero gap, and the separation between the two trucks varies in the range 0-1.7$\sqrt{A}$. Individual truck models are characterized by their measured drag behavior in isolation rather than by their detailed geometry.

The results demonstrate that two trucks in tandem always present less drag than the same two trucks operated in isolation. The saving in drag depends upon the value of the truck drag coefficient in isolation. When an aerodynamically clean truck and an aerodynamically dirty truck are operated in tandem, it is always better to place the clean truck in front. Very roughly, for spacing less than about 0.5$\sqrt{A}$, the total drag saving (both trucks) is of the order of 30%. For spacing greater than 1.0$\sqrt{A}$, the total drag saving is of the order of 20%. For modest changes in drag, the change in fuel consumption is linearly proportional to change in drag. The constant of proportionality depends upon truck parameters and driving schedule, but might realistically lie in the range 0.5-0.75.

Aerodynamic Forces on Truck Models, Including Two Trucks in Tandem

I Desires for Greater Fuel Economy, Less Pollution and Greater Safety

Federal government Involvement

The increasing quantity of fuel consumed by large trucks traveling the highways of the nation is a major concern for the federal government. Currently, imported oil accounts for approximately 10 million barrels per day of the total daily consumption of 19 million barrels. Roughly 9 million barrels per day are consumed by road vehicles, and of this 9-million-barrel total, about two million barrels are consumed by class 7 and 8 trucks—the fastest growing segment of interstate vehicular traffic. In an effort to reduce the nation's dependence on foreign oil, a program termed the *21st Century Truck Initiative* is planned as a partnership between the federal government and the truck industry. The objective is to significantly increase the fuel economy of class 8 trucks, transit buses, class 6 delivery vans and class 2b pickups (LA Times, February 2000).

Heavy trucks and buses have recently come under increased scrutiny from environmental groups concerned about the health hazards of particulate emission by large diesel engines. For example, according to a recent Los Angeles Times article, large diesel engines in trucks (and buses) account for one-quarter to one-half of the soot and nitrogen oxides emitted from all vehicles including private cars (LA Times, May 17, 2000)

The roadmap developed by the DOE for the *21st Century Truck* recognizes that more than half the fuel consumed by large trucks on the highways serves to overcome aerodynamic drag. Thus both a significant saving in fuel consumption and a significant pollution abatement can be achieved by decreasing aerodynamic drag.

Private Company Involvement

The potential for fuel savings due to drag reduction has not been lost on the truck manufacturers. A simple and effective way to reduce drag and hence reduce fuel consumption is to allow one tractor-trailer to be closely followed by a second tractor-trailer. Daimler-Chrysler terms this concept the Electronic Tractor Hitch (ETH) since the concept would necessarily involve automatic control of throttle, brake and steering. On June 17, 1999*, Zeit* reported a presentation made to a number of journalists.

> "With this device (ETH), two trucks are coupled by an infrared system. The driver of the second truck can rest while driving at full speed. Harmut Marwitz, DC's chief truck designer, believes that it is possible for trucks to couple and decouple on the highway—thus building Australian-like road trains (or platoons) in which the duty of steering remains with the first truck." … "the ecological advantage of fuels savings in the range of 10-15% is noted by DC's Marwitz. Interestingly, experiments have shown that at separations below 8 meters, the forward truck saves more fuel than the trailing truck. With fuel costs in Europe of approximately $35K per truck per year, a 10-15% saving is considerable. After 18 months of operation, the ETH should reach a break-even point, and the truck owners begin to save money. In this win-win strategy, both truck owners

and manufacturers of ETH benefit. Polls show that 65% of truck owners would be interested in purchasing such a system."

Fuel costs in the US are, of course, lower than in Europe, but a typical tractor may log 175,000 miles per year. Assuming an optimistic fuel price of $1.50 per gallon, the resulting fuel costs per tractor in this country are of the order of $40,000 per year.

Caltrans/PATH/USC Involvement

The present study is part of a larger scale research effort, sponsored by The California Department of Transportation (Caltrans) and the PATH Program at UC Berkeley, to provide means for safe and more efficient use of California highways. Much of the recent work has focussed upon the transportation of people and goods by large vehicles, and considers the feasibility of operating truck or bus platoons of two or three closely spaced vehicles. The culmination will be a truck platoon and a bus platoon demonstration—termed DEMO 2003—to take place on interstate I-15 just north of San Diego in the summer/fall of 2003.

Single truck safety issues are also important. While the number of highway traffic deaths per passenger mile has declined for passenger vehicles over the past 25 years, the number has remained almost constant for accidents involving heavy vehicles (see LA Times, May 26, 1999). Many of the sensors necessary for platoon travel could easily serve a broader purpose by providing the early warning of an impending collision. Also, by utilizing the various sensor outputs—in connection with a proper dynamical system model—the automatic throttle, braking and steering systems could be programmed to behave intelligently during the severe maneuvers necessary for collision avoidance.

The present wind tunnel experiments (and planned follow-on experiments) provide 6-component force and moment measurements for a single cab and trailer. Forces and moments are measured separately on the cab and on the trailer. Independent measurements are important since the cab and trailer are separate, but dynamically linked, bodies. In the tests, forces are measured as a function of the cab-trailer gap separation and the yaw angle between the relative wind and the axis of the cab-trailer model. The yaw angle is meant to account for the presence of an over-the-road side-wind. The present data set is unique in providing force information separately for cab and trailer, and in spanning the 2-dimensional parameter space of cab-trailer gap separation and yaw angle.

The present (and planned) wind tunnel experiments also provide drag information for two trucks in tandem. The measurements employ not just a single truck shape, but a variety of simple truck shapes. These individual truck shapes are characterized by their measured drag behavior in isolation (and not by their particular geometry), as discussed in sections II and III. The results can be widely disseminated and used to estimate fuel savings for a variety of over-the-road scenarios. Several fuel saving scenarios are illustrated in section IV.

II Predicting Force and Moment Behavior from Wind Tunnel Tests

Similitude

Equipment manufacturers commonly use wind tunnels tests during the design process. The desire is to predict the performance of the full-scale truck from the measurements on scaled models. This is a formidable task, and often designers are content to measure the performance of one model design *relative* to other designs. For perfect *geometric similitude* between a wind tunnel model and a full-scale truck, the model must be similar in all detail to the full-scale truck—including mounting the model on a moving ground plane in the wind tunnel, allowing the wheels to roll on the ground plane, and allowing for flow within the engine compartment. Such model-building and testing would be prohibitively expensive, and most wind tunnel tests are performed on models that are less than perfectly detailed—for example, they are often geometrically simpler, and have fixed wheels and rest on a stationary ground plane. Allowances or corrections can sometimes be made for imperfections in *geometric similitude*.

Examination of the equations describing the aerodynamic flow predicts that the *size* of the model is not itself important, but rather the *product of size and speed*. Thus the behavior of a full-scale truck traveling at 50 miles per hour is in every respect equivalent to the behavior of a ½-scale truck model tested in the wind tunnel at 100 miles per hour. This requirement is sometimes termed *dynamic similitude or Reynolds number similitude*. Small models can be used, but only to a limited extent since the velocity would have to be increased accordingly. In cases where small model size does not allow perfect *dynamic similitude* to be achieved, some measure of the *sensitivity* of the results to changes in Reynolds number may still be obtained by testing at different wind tunnel speeds.

Presence of Wind Tunnel Walls

Most low turbulence wind tunnel test sections are enclosed as is our Dryden wind tunnel. The presence of the wind tunnel walls surrounding the test section pose an additional problem for modelers, since walls obviously do not exist in the full-scale situation. In the strictest sense, the two situations cannot be compared because they are geometrically different. However, if the walls are not too close, a correction—or better yet, an extrapolation—can be applied to the wind tunnel measurements to approximate the flow in the absence of walls.

These corrections (extrapolations) are generally referred to as “blockage corrections” for the following reason. Imagine marking parcels of air on an imaginary boundary surrounding the truck and approaching from upstream. The stream surface traced out by the moving parcels of air must necessarily expand in size as the air flows around the truck. If the wind tunnel walls were to lie along such a stream surface, they would present no harmful effect. This, of course, would require the walls to be moveable to accommodate different models, and some means would need to be provided to verify that the walls are indeed aligned along a stream-surface of the undisturbed flow. A few such wind tunnels exist. They are termed adaptive-wall wind tunnels.

When the correct stream surface is replaced by straight walls enclosing a fixed cross-sectional area, as in a conventional wind tunnel such as our Dryden tunnel, the walls will unduly constrain the flow in the vicinity of the model. Simple continuity suggests that velocities over the model will be increased above values that would occur in the absence of walls, and lead to a

measurement of drag that is too high. A possible correction procedure would be to regard the drag measurement to be correct—provided one utilizes, as a measure of speed, the velocity

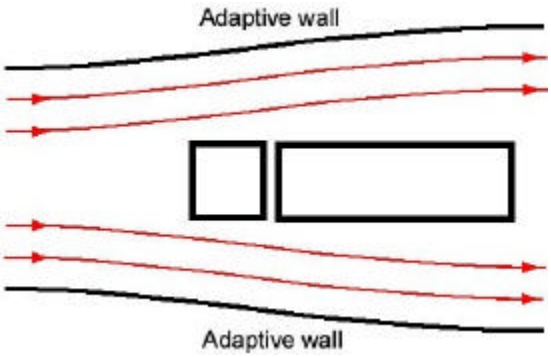

Figure 1a Adaptive wall wind tunnel.

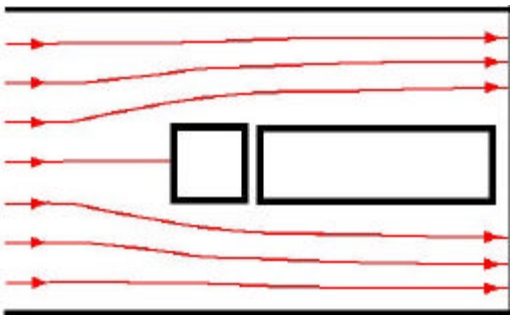

Figure 1b Conventional wall wind tunnel.

in the vicinity of the model and not the speed in the flow upstream of the model. This leads to a corrected drag coefficient

$$C_D = D_{measured}/(A*q_c),$$

where $D_{measured}$ is the measured drag, A is the cross-sectional area of the model, and q_c is the corrected dynamic pressure in the vicinity of the model. The quantity q_c can be related to the dynamic pressure, q_∞, in the upstream (undisturbed flow) by a variety of means. One simple choice is to utilize the steady flow continuity relation to argue that velocity, U_c, is increased above the measured upstream value, U_∞, by the ratio of areas available to the flow.

$$U_c = U_\infty*(A_\infty/(A_\infty-A)),$$

where A/ A_∞ is the ratio of model cross-sectional area to empty tunnel area. Also, then

$$q_c = (U_c/ U_\infty)^2*q_\infty.$$

A detailed discussion of blockage corrections can be found in the SAE Publication SP-1176 (Cooper, 1995). Many of the correction procedures are quite elaborate, and require considerable additional information about the flow. Generally speaking, blockage corrections are rarely applied for blockage ratios less than 2 per cent. They make sense for blockage ratios up to 5 per cent perhaps. At 10 per cent blockage, the corrections (extrapolations) would be of the order of 20 per cent and are too large for accurate drag determination.

Categorizing Trucks by Drag Coefficient

Our approach to the problem of imperfect similitude is somewhat different. We shall not attempt to make precise comparisons between trucks of slightly different geometry. Rather, we regard the drag coefficient as the parameter of defining interest, and classify trucks according to their drag coefficients in isolation. Thus the detailed truck shape is not important from our point of view, but the drag coefficient is important in defining the aerodynamics of any particular model. Our basic truck model is relatively simple in shape (see Section III). The drag of this simple

shape can be increased by the addition of one or more of: thin surface netting over the cab (10% drag increase); “collars” installed near front of the trailer to increase boundary layer thickness and drag (9% increase); wheels (25% increase); and a 15% mismatch between cab height and trailer height (9% drag increase). We can then operate various of these models at yaw, or various combinations of models in tandem with some expectation that the results will be appropriate for full-scale trucks exhibiting similar drag coefficients in isolation.

Since force coefficients are to be applicable to trucks operating on the open road, it is still necessary to correct our measured (coefficient) values for wind tunnel blockage, The correction method described in the preceding section is termed the “continuity” correction, and the performance is documented—among other methods—in SP-1176. The continuity method suffers to some extent because the degree of blockage does depend upon the model shape as well as the cross-sectional area, and this additional dependence is not accounted for in the method. We make an important improvement to the continuity method by making use of a static pressure rail running the entire length of the test section ceiling to determine the values of the local velocity. The value of the dynamic pressure, q_c, is taken to be the values measured at the test section ceiling averaged over the length of test section occupied by the model. The correction can be applied equally well to cab and trailer separately when data for both are available. The correction can also be applied separately, and without confusion, to each truck in a tandem truck arrangement.

III Description of Models and Test Conditions

The Wind Tunnel Models

Models are constructed from Spyder foam (2.2 #/ft^3). Spyder foam is a high density machinable styrofoam that we cut under computer-control in a three-axis routing machine, or light-duty milling machine. A dimensioned three-view drawing of the cab and trailer is presented in Figure 2. Each half of each cab or trailer is machined separately. Later, the halves are epoxyed

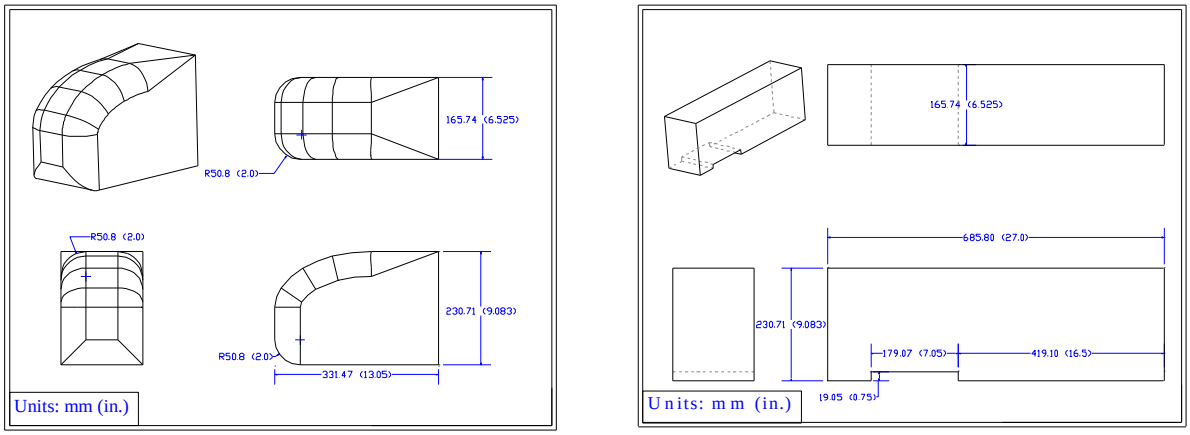

Figure 2 Three-view drawing of cab and trailer used in wind tunnel experiments.

together, and aluminum end plates and an aluminum underplate—necessary to support the force sensor—are added. The cab shape bears little resemblance to any real truck design. The main feature is an elongated and rounded nose having a radius of curvature of 50 mm for the vertical forward edges. This radius is chosen to insure that premature separation does not occur over the cab at the Reynolds numbers achievable in our wind tunnel tests. The criterion is that the Reynolds number—based upon edge radius—should exceed a value of about 70,000 (Cooper, 1985),

$$Re_\eta = U_\infty \eta / \nu \geq 70{,}000,$$

where U_∞, η, and ν are respectively: undisturbed wind tunnel speed (m/s), edge radius (m), and kinematic viscosity (m^2/sec). The cross-sectional area, or frontal area of the models is A = 0.0382 m^2. The square root of this area—sometimes given the symbol $\sqrt{A}$ = 0.1955 m = 195.5 mm—is used as a length scale to non-dimensionalize the gap between cab and trailer and the separation between two trucks in tandem.

Elements are added to the basic model of Figure 2 to increase the drag. These various additional components can be seen in the side-views of Figure 3. The associated drag coefficients (not corrected for blockage) are shown on the right. A polypropelene netting,

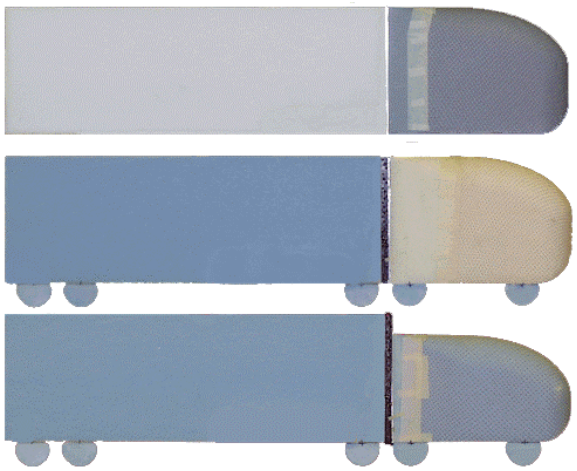

Drag Characteristics	$C_{Disolation}$
"Clean truck" • No wheels • No drag collar • Netting	C_{Diso} = 0.427
"Dirty truck" • Wheels – 20% • Drag collar – 9% • Netting	C_{Diso} = 0.544
"Mismatch truck" • 15% height difference – 9% • Wheels – 20% • Drag collar – 9% • Netting	C_{Diso} = 0.586

Figure 3 Various truck models and their drag characteristics.

designated (N), is usually placed over the nose of the cab extending to within three centimeters of the rear of the cab. This serves to increase the drag of the unadorned model by about 10%, but has the greater purpose of insuring that the boundary layer is made turbulent before the flow reaches corners and edges where separation is to be avoided. Wheels, denoted (W), can be added (or removed) by means of double-sided adhesive tape. To provide additional drag, a removable collar consisting of many, small protruding cylindrical elements (each of 120 cylinders on the collar is 3.2 mm in diameter and 19 mm in length) is added. The collar, denoted (C), is placed at the forward end of the trailer where it serves to create an additional generalized momentum deficit. A cab having a shortened height of 195.3 mm is meant to model cabs and trailers that are mismatched in height. The mismatched cab, denoted (MM), is shown in the lowest portion of Figure 3.

Finally, a model having a separated cab and trailer is designed to be tested over a range of yaw angles. The scale of this model is 10 percent smaller than previous models, and the trailer is slightly shortened to decrease the wind tunnel blockage experienced at large angles of yaw. The dimensions of the model are shown in Figure 4. The geometry is similar to the previous models except that the front of the trailer has rounded vertical edges of radius 45 mm. The edge rounding is meant to correspond more nearly to a real trailer. Together, the cab and trailer have a total length of 983 mm at zero separation, corresponding at full scale to a length of about 16.5 m (54.3 feet). Here the model is tested with wheels (W), and netting (N) over the cab.

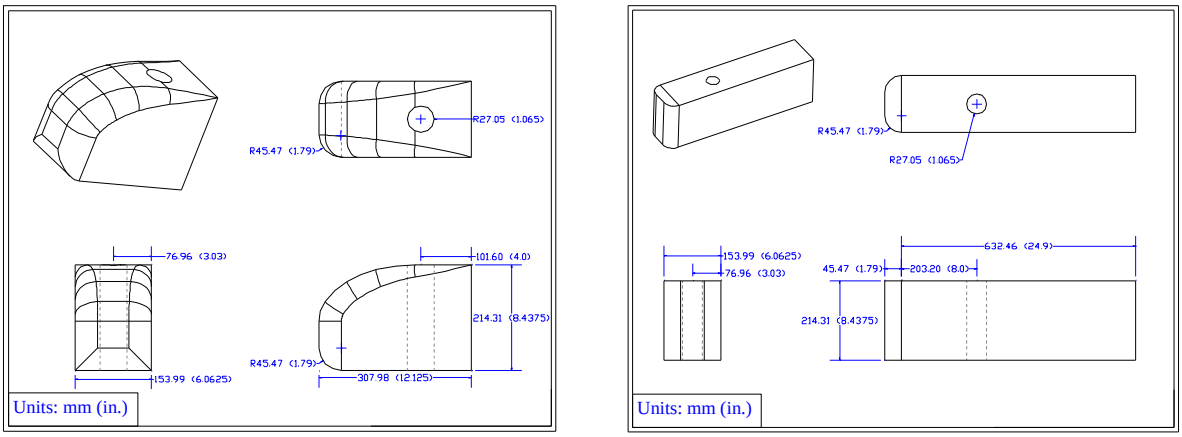

Figure 4 Single cab and trailer with trailer attachment having rounded vertical edges.

Force and Moment Measurement

For the measurement of the drags of two trucks in tandem, each truck consists of a rigidly connected cab and trailer. Each truck is supported upon an internal force balance capable of measuring drag in the range –14 to +14 N. For the trucks in tandem at zero yaw angle, side forces and yawing moments are very small and are of no consequence. Each force balance rests flush with the bottom of the truck, and is connected by two thin stainless steel posts to a stepper-motor-controlled carriage below the ground plane. The trailing or rear truck, denoted (R), can be moved with respect to the lead or forward truck, denoted (F).

The single cab and trailer are designed to carry newly purchased six-component force balances. These balances are smaller, and measure forces to approximately $\pm$ 200 N. Although all components of force and moment are available, only drag, side-force and rolling moments measured separately for cab and trailer will be presented here for a range of yaw angles. In this case, the separation between cab and trailer is an additional variable. The trailer moves relative to the fixed cab, and both the cab and trailer carriages rest upon a stepper-motor-controlled yaw turntable. Data is recorded for yaw angles between 0 and 16 degrees. (Measurement over a larger range of yaw angles is presently being planned.)

The wind tunnel data is presented in coefficient form, by dividing the measured force values by model cross-sectional area and dynamic pressure, as follows.

$$C_D = D_{measured}/A*q \quad \text{or} \quad D_{measured}/A_W*q$$

$$C_{SF} = (SideForce)_{measured}/A*q \quad \text{or} \quad (SideForce)_{measured}/A_W*q$$

$$C_{Roll} = (Roll\ Moment)_{measured}/A*\sqrt{A}*q \quad \text{or} \quad (Roll\ Moment)_{measured}/A_W*\sqrt{A}*q$$

The value A is the cross-sectional area of the trailer (identical to the cab). If the model has wheels attached, the projection of the wheels is included in the cross-sectional area, A_W . Wheel area is not included in the length measure $\sqrt{A}$. The value of dynamic pressure q, either refers to the undisturbed free-stream value, q_∞, or to the value corrected for blockage, q_c. Drag is positive in the downstream direction. When the cab and trailer are yawed, side force, or side force coefficient is taken to be positive when the force acts to push the truck from the windward side toward the leeward side. Rolling moment is measured about a longitudinal axis midway between the upper surface and the lower surface of the trailer (the trailer mid-plane), and is taken positive when the top of the trailer rolls toward the leeward side.

The data discussed here for the yawed cab and trailer and for the tandem trucks was recorded during the latter half of 2000. The tests usually extend over a 3-4 week period. Force balances are “re-zeroed” about every half hour, and are re-calibrated as needed. They are inherently linear (strain gage) devices, and insuring proper gain settings and proper “zero force” settings are sufficient to obtain accurate force measurement. A measure of the repeatability of the forces can be judged from several of the truck-in-isolation drag results logged over a several-week period, and shown in the following table. The configuration is given in the left column. For example, RWCN is short-hand for truck with (W)heels, (C)ollar and (N)etting in the position of the (R)ear truck in the wind tunnel. Trailer skirts are always used to cover the exposed edges of the force balances, although they are not depicted in Figure 3. The configuration F+2S refers to a single truck in forward position, and with two additional trailer skirts taped to the sides of the trailer. Skirts are shown to make a negligible contribution to the drag. Note the drag coefficient,

C_D, is uncorrected for blockage. The final four entries are drag values for the single cab and trailer ((W)heels, (N)etting, and a trailer with rounded vertical edges) at zero yaw and zero separation. If a particular configuration is tested repeatedly, the average for all similar configurations is given in the column labeled C_{DAv}.

Name	Drag N	Velocity m/s	q_∞ Pa	Ref Area m^2	C_D	C_D av	Blk_Fac	C_D/Blk
RWCN	7.69	24	353.93	0.0419	0.519	0.523	1.059	0.494
FMMN	6.29	24.2	359.85	0.0383	0.456		1.063	0.429
FMMCN	7.08	24.25	361.34	0.0383	0.512		1.065	0.480
FN	6	24.2	359.85	0.0383	0.435	0.427	1.062	0.402
FCN	6.55	24.2	359.85	0.0383	0.475	0.467	1.067	0.438
FMMWCN	8.98	24.4	365.82	0.0419	0.586		1.07	0.548
FWCN	8.21	24.2	359.85	0.0419	0.545	0.544	1.072	0.508
FWCN	8.23	24.25	361.34	0.0419	0.544		1.072	0.507
FCN	6.33	24.2	359.85	0.0383	0.459		1.067	0.430
FCN+2S	6.33	24.25	361.34	0.0383	0.457		1.067	0.429
FN+2S	5.79	24.3	362.83	0.0383	0.417		1.062	0.392
FN	5.78	24.2	359.85	0.0383	0.419		1.062	0.395
F	5.43	24.35	364.32	0.0383	0.389		1.057	0.368
F+2S	5.44	24.35	364.32	0.0383	0.390		1.057	0.369
RWCN	8.06	24.4	365.82	0.0419	0.526		1.059	0.497
RWCN	7.87	24.15	358.36	0.0419	0.524		1.059	0.495
RN	5.86	24.2	359.85	0.0383	0.425		1.048	0.406
RCN	6.37	24.15	358.36	0.0383	0.464		1.052	0.441
CAB/WN	6.83	26.62	435.42	.03605	0.435	0.430	1.050	0.414
TRLR/WN	2.05	26.62	435.42	.03605	0.131	0.135	1.087	0.120
CAB/WN	6.77	26.77	440.17	.03605	0.426		1.049	0.406
TRLR/WN	2.20	26.77	440.17	.03605	0.138		1.086	0.127

The differences in measured drag between individual realizations of the same geometry are about ≈0.01 in terms of drag coefficient. For example, configurations FCN and FN show a difference between two realizations of about 0.016, although all of the other repeated tests have smaller differences. The last two columns provide a correction factor for wind tunnel blockage and a corrected value for the drag coefficient, as discussed in a later section entitled *Blockage Correction*.

Model Alignment and Positioning

When two trucks are run in tandem, they are installed and aligned as follows. The rear truck (R) is first mounted on the yaw turntable, and aligned with the free stream by incrementing the yaw angle until side force and yawing moment are essentially zero. This can be accomplished to an angular accuracy of about ±0.05 degrees. The forward truck (F) is then mounted in a separate fixture ahead of the yaw turntable. This fixture allows for lateral translation of the truck, and for a slight yaw angle correction. The forward truck is then positioned directly in front of and parallel to the rear truck as viewed by an observer standing upstream in the contraction section of the wind tunnel. Straight edges placed along the truck sides confirm this alignment. At “zero spacing” the trucks are 12.7 mm apart. The stepper motor controlling the position of the rear

truck is programmed in LabView to move downstream in 20 mm steps. There are a total of 16 steps, corresponding to a maximum separation of 332.7 mm, or 1.67$\sqrt{A}$. The rear truck is then brought back to zero spacing in the same 20 mm increments.

For the single truck to be tested a yaw, the cab and trailer are mounted in separate fixtures on the yaw turntable. In this case separation between cab and trailer is produced by stepping the trailer rearward. The position of "zero spacing" corresponds to a separation of 2 mm, and there are a total of 20 positions at increments of 10-20 mm for a total separation of 282 mm. The trailer is then returned to zero spacing by the same sequence of increments. Cab and trailer are yawed as a unit through 21 steps of 1 or 2 degrees. The traverse sequence is begun at zero yaw and "zero spacing", and stepped through all spacings. The most negative yaw angle is next established, and the same separations are sampled. Sampling continues for all negative yaw angles—passing through zero yaw to +2 degrees and returning to a final zero yaw position.

Tests for Reynolds Number Sensitivity

Sensitivity to changes in Reynolds number (Reynolds number similitude) is monitored by repeating the tests at different wind tunnel speeds—typically at three or four speeds spanning the range from 16 m/s to 26 m/s. This corresponds to a range of Reynolds numbers from 210,000 to 336,000, if Reynolds number is defined as $U_\infty * \sqrt{A}/\nu$. This is not a particularly large span of Reynolds number: nevertheless it serves to identify any unforeseen peculiarities present in the data. None are observed, and the dependence of force coefficients on Reynolds number over this range of Reynolds numbers is minimal.

Pressure Surveys

The static pressure distribution along the test section ceiling is recorded at predetermined times during the force measurement. There are a total of 35 pressure taps spaced at intervals of 152.4 mm. These local static pressures are output in the form of a local pressure coefficient—that is, the static pressure relative to the static pressure measured upstream at a fixed reference point and normalized by the dynamic pressure at this same reference point, $C_p = (p-p_\infty)/q_\infty$. Individual pressures are output to a Baratron through a Scani-valve pressure sequencer. A second Baratron continuously monitors the upstream dynamic pressure, q_∞.

Data Acquisition

Signals from all the force balances (and the Baratrons) are digitized with 12 bit accuracy under LabView control—usually at the rate of 1 K digitizations per second. It is common to average the outputs over an 8-second interval ($\approx$ 8000 digitizations). In the case of the force balance data, the voltages are translated into forces by use of a calibration matrix (a 3x3 matrix for each of the older, 3-component balances, and a 6x6 matrix for the newer balances) determined earlier by dead-weight calibration and stored in the computer. Outputs are placed in a memory buffer, and written to disk at the end of each run. For the two trucks in tandem, a run consists in incrementing the separation from zero to maximum separation and returning to zero separation. Each run takes about 35 minutes to complete, and there are some 62 runs in this data set—representing a total testing time of about 36 hours. For the single truck at yaw, a run consists of incrementing the yaw angle from zero through positive angles to maximum yaw, returning

through increments to a specified negative yaw angle, and then returning through increments to zero yaw. The data set for the single truck at yaw represents a total wind tunnel running time of about 24 hours.

Blockage Correction

If force coefficients determined from wind tunnel data are referenced to the undisturbed dynamic pressure ahead of the model, the force coefficients will be over-predicted. As explained in Section II, the presence of wind tunnel walls increases flow velocities in the vicinity of the model and therefore increases the drag above values measured in the absence of walls. The correction for blockage consists in determining a velocity (or dynamic pressure) more characteristic of the values in the vicinity of the model. This value of the dynamic pressure, q_c, is taken to be the average of values measured at the test section ceiling over the length of test section occupied by the model. The procedure is illustrated as follows. The local pressure at any position along the test section ceiling is recorded in the form of a pressure coefficient, C_{pl}.

$$C_{pl} = (p_l - p_\infty)/q_\infty \equiv 1 - (U_l/U_\infty)^2$$

Thus,

$$q_l/q_\infty \equiv (U_l/U_\infty)^2 = 1 - C_{pl}$$

Averaging over the x-positions occupied by the model gives,

$$<q_l>/q_\infty = <1 - C_{pl}> \equiv q_c/q_\infty = 1 - <C_{pl}>$$

And finally, the drag coefficient, for example, is given by

$$C_{Dcorr} = D_{measured}/q_c*A = D_{measured}/[A*q_\infty*(1 - <C_{pl}>)]$$

The quantity q_∞ is recorded at the time of measurement, and the factor $(1 - <C_{pl}>)$ is determined from any previous pressure scan with the model (or models) in identical position(s) in the wind tunnel. Such a pressure scan is shown in Figure 5 for the case FWCN24—corresponding to a single truck with wheels, drag collar and netting at a nominal speed of 24 m/s and located in the forward position in the wind tunnel. Figure 5 shows the difference between the empty tunnel static pressure signature and the pressure signature with the model present. The physical

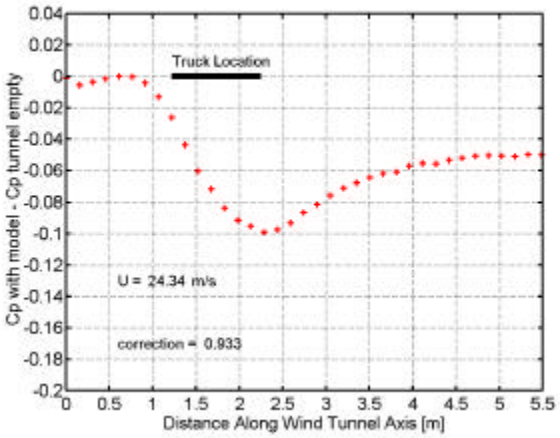

Figure 5 The difference between tunnel pressure scan for empty tunnel and tunnel with model (Case FWCN24).

location of the model is the darkened bar indicated on the plot. The presence of the model produces a local decrease in C_p—corresponding to a local increase in speed. The maximum (negative) increment in C_p is about -0.10 coincident with the location of the rear of the trailer. Note also that the pressure signature does not return to zero because of the presence of a wake downstream from the model. For this case, $\langle C_{pl} \rangle$, averaged over the model position, yields the value -0.0717. The correction factor, $1/(1-\langle C_{pl} \rangle)$, is 0.933.

IV Results

Drag, Side Force, and Rolling Moment for the Cab and Trailer at Yaw

The global features of the most important force coefficients on the cab and trailer are shown separately in Figures 6-12. Since coefficients for cab and trailer are referenced to the same cross-sectional area, the total force coefficient is obtained by simple addition of the two. The non-dimensional range of cab-trailer separations is from 0-1.6, and the yaw angle range is 0-16 degrees. The angle range represents a fair sampling of common wind speeds and directions (with respect to the moving truck), but it does not include many interesting extreme wind conditions. More extreme conditions will be examined in a follow-on experiment. Figure 6 and 7 present the cab drag coefficient and the cab drag coefficient corrected for wind tunnel blockage. These two figures are very similar; the blockage correction lowers the uncorrected

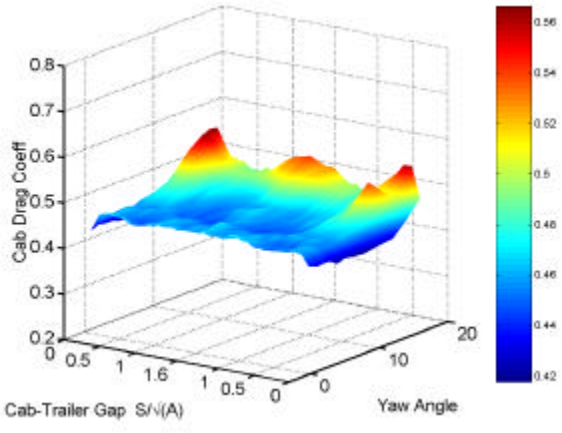

Figure 6 Cab drag force coefficient versus cab-trailer gap and yaw angle.

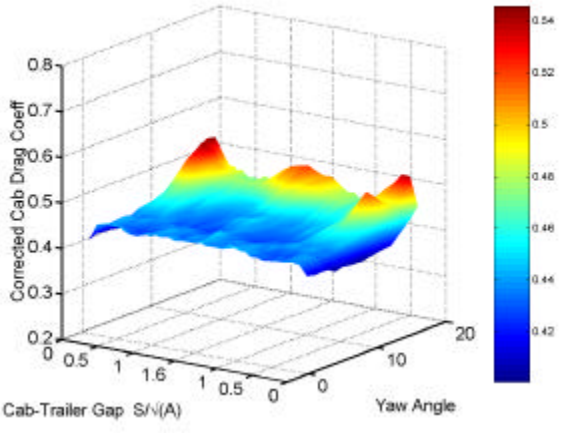

Figure 7 Corrected cab drag force coefficient versus cab-trailer gap and yaw angle.

drag value more-or-less uniformly over all spacings and yaw angles. This is true for all the coefficients, and the remaining figures show only the corrected values. From Figure 7 it can be seen that cab drag is relatively independent of both spacing and yaw angle for small yaw angles. The "drag plane" is more-or-less featureless out to yaw angles of the order of 6-8 degrees. Then there arises a prominent cab drag peak at a particular spacing of between $0.25\sqrt{A}$-$0.5\sqrt{A}$. As the spacing increases (at fixed yaw angle) beyond this peak, the drag actually falls. The spacing associated with the drag rise should be avoided in practice. The explanation for this curious sensitivity is still not completely clear, but it is associated with the existence of a strong cross-flow that arise spontaneously within the gap. In contrast, Figure 8 shows that trailer drag coefficient increases strongly with increasing separation and with increasing yaw. Drag is least—and considerably smaller than the cab drag—at short spacing and small yaw angle. The small value is due to the shielding of the front of the trailer by the cab.

There is a considerable increase in side force coefficients for both cab and trailer (Figures 9 & 10) with increasing yaw angle, but remarkably little dependence on spacing. It is also remarkable that the side forces on the cab and trailer have about the same magnitude in spite of the much greater length of the trailer.

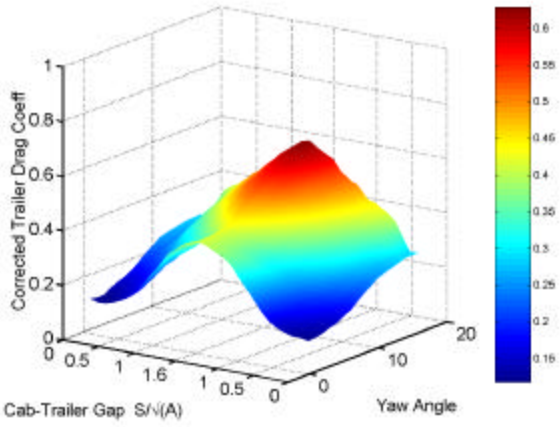

Figure 8 Corrected trailer drag force coefficient versus cab-trailer gap and yaw angle.

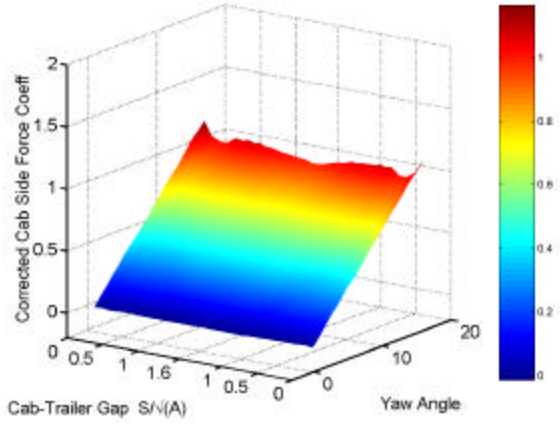

Figure 9 Corrected cab side force coefficient versus cab-trailer gap and yaw angle.

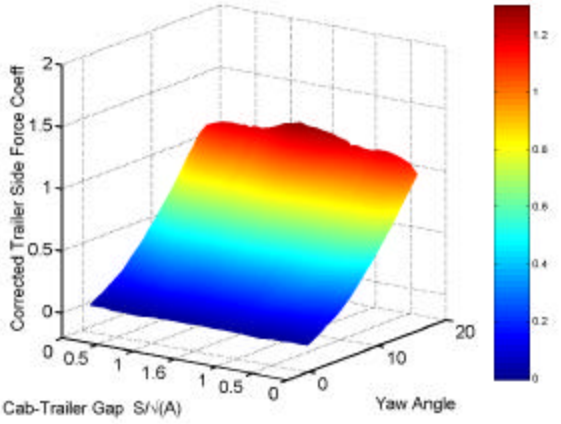

Figure 10 Corrected trailer side force coefficient versus cab-trailer gap and yaw angle.

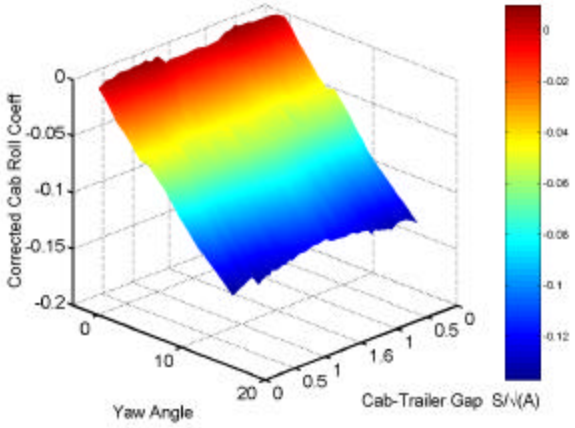

Figure 11 Corrected cab roll coefficient versus yaw angle and cab-trailer gap.

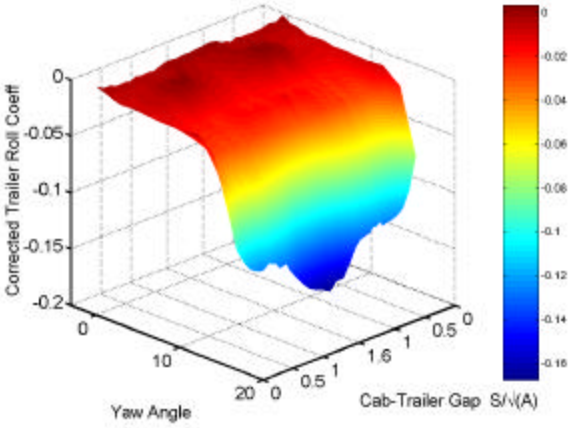

Figure 12 Corrected trailer roll coefficient versus yaw angle and cab-trailer gap.

Figure 11 shows that the cab rolling moment is zero at zero yaw (as it must be) and increases steadily with increasing yaw angle. It is nearly independent of the spacing between cab and trailer. Remember that rolling moment is taken about a central axis at the mid-plane height of the cab (or trailer). The increasingly negative value of rolling moment with increasing yaw simply means that the line of action of the side force lies slightly below the mid-plane height. Trailer roll coefficient (Figure 12) is also relatively independent of spacing between cab and trailer, but trailer roll coefficient increases sharply at an angle of about 10 degrees of yaw.

These dependencies are observed more quantitatively by plotting cuts through the two-dimensional surfaces. A number of such cuts are shown in Figures 13-15. Again, all the coefficients are corrected for wind tunnel blockage as determined earlier. Figure 13 (a), (b), present drag coefficients as a function of spacing, respectively, for the two yaw angles, yaw = 0 and yaw = 16 degrees. In each case, the red crosses are for the trailer, blue crosses represent

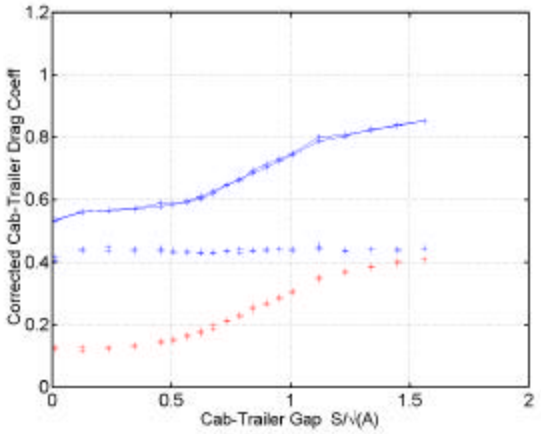

Figure 13a Corrected cab-trailer drag force coefficient versus cab-trailer gap at 0º yaw.

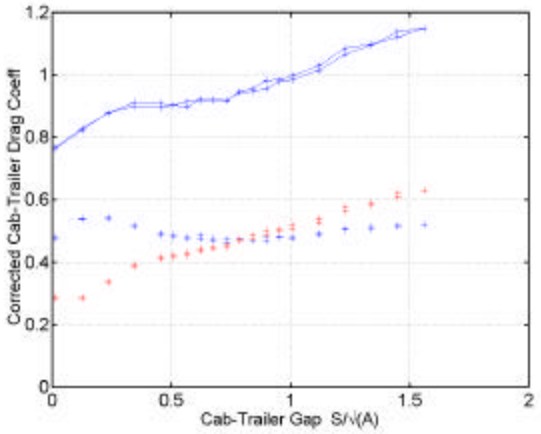

Figure 13b Corrected cab-trailer drag force coefficient versus cab-trailer gap at 16º yaw.

the cab, and the sum is plotted with a superimposed blue line. The two crosses at each spacing represent the data points obtained for spacing increasing from zero to a maximum, then decreasing from the maximum spacing to zero. At zero degrees of yaw, the cab drag is nearly independent of spacing, although a small rise in the region $0.2\sqrt{A}$-$0.4\sqrt{A}$ can be discerned. At 16 degrees yaw, the relative peak in cab drag coefficient is more evident at a spacing of about $0.25\sqrt{A}$. The additional drag produced by the cab is also evident in the sum, although the drag continues to rise as a result of increasing trailer drag.

Figure 14 (a), (b), (c) respectively present drag, side force and rolling moment as a function of yaw angle at zero spacing. Figure 15 (a), (b), (c) give the same information for a nondimensional spacing of 1.45. These curves demonstrate the features already discussed, including the large side force coefficient at large yaw. Note that the side force appears to increase linearly with yaw angle up to about 5 degrees, and then to increase more rapidly at larger yaw angles.

The more rapid-than-linear increase in side force is almost certainly due to the appearance of large vortices on the leeward side of the truck at an angle of yaw of about 5 degrees. The aerodynamic situation is analogous to that of a low aspect ratio wing at an angle of attack, where it is known that vortices are shed from the wing edges, and promote additional lift. In our case, the truck itself (cab plus trailer)—and its image below the ground plane—is the low aspect wing, and yaw angle can be equated to angle of attack.

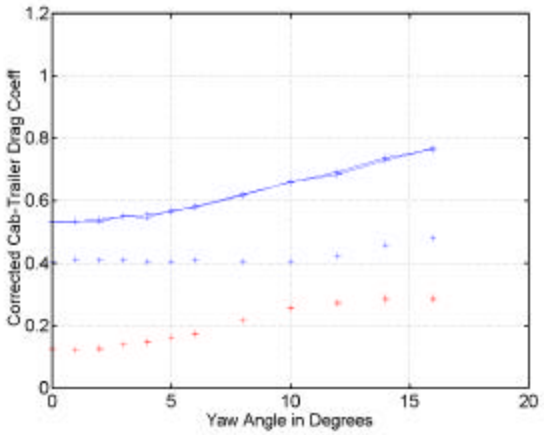

Figure 14a Corrected cab-trailer drag force coefficient versus yaw angle at 0 spacing.

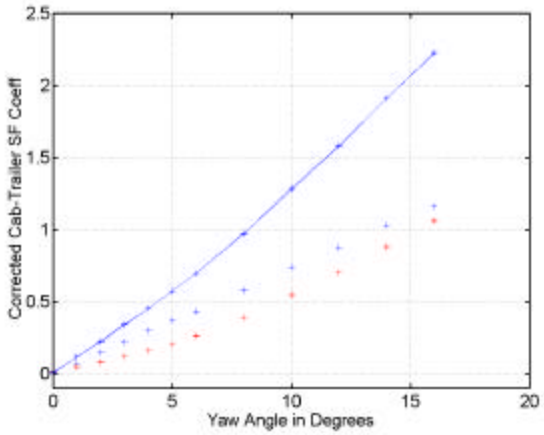

Figure 14b Corrected cab-trailer side force coefficient versus yaw angle at 0 spacing.

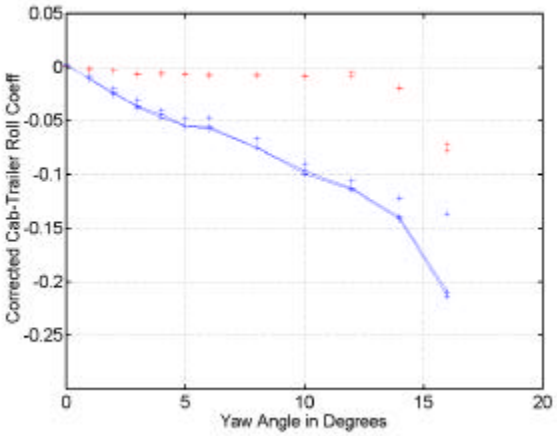

Figure 14c Corrected cab-trailer roll coefficient versus yaw angle at 0 spacing.

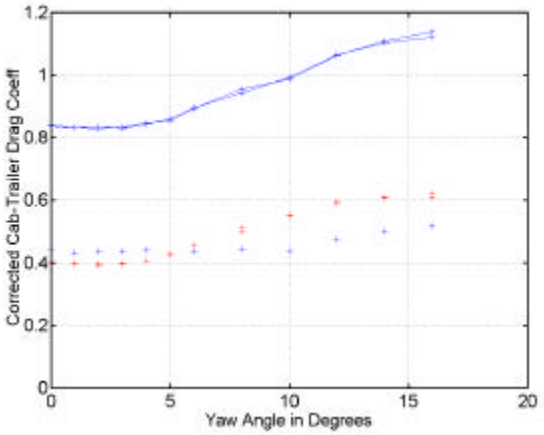

Figure 15a Corrected cab-trailer drag force coefficient versus yaw angle at 1.45 spacing.

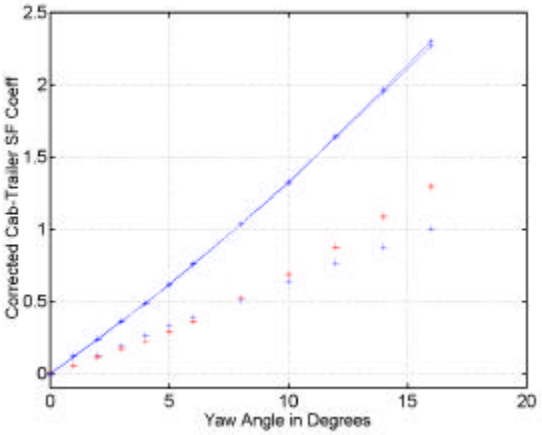

Figure 15b Corrected cab-trailer side force coefficient versus yaw angle at 1.45 spacing.

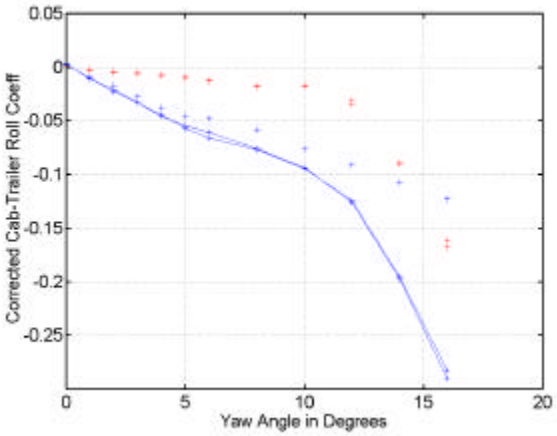

Figure 15c Corrected cab-trailer roll coefficient versus yaw angle at 1.45 spacing.

The side force and rolling moment results can be combined to determine the side force line-of-action. Recall that the rolling moment is resolved around an axis through the horizontal trailer (cab) mid-plane. The rolling moment is negative (Figures 11 & 12), meaning that the physical line-of-action of the side force lies below the trailer (cab) mid-plane. If this distance is defined as Z_{CP}, then

$$Z_{CP}/\sqrt{A} = -C_{Roll}/C_{SF}$$

For the cab, $Z_{CP}/\sqrt{A}$ remains in the vicinity of 0.11-0.12 over the entire range of cab-trailer gaps and yaw angles. For the trailer, $Z_{CP}/\sqrt{A}$ is 0.03-0.05 for all gaps at yaw angles below 10 degrees, but increases to the range 0.11-0.12 at gaps $\approx$ 1.45 and yaw $\approx$ 16°.

Drag for Two Trucks in Tandem

The final seven figures summarize drag data for two trucks operating in tandem. The term truck refers to a cab plus a trailer without a gap (separation between cab and trailer). The truck can be in one of three configurations: Clean (Netting, no Wheels no Collar, no cab height MisMatch); Dirty (Netting, Wheels, Collar, no MisMatch); or Dirty with MM (Netting, Wheels, Collar MisMatched cab), as illustrated in Figure 3. Truck separation here refers to the distance between the two trucks, normalized by the square root of the truck cross-sectional area. For example, Figure 16 gives drag coefficients for the combination Dirty Lead/Dirty Trail. In this case, both trucks are identical. The ordinate represents the truck drag ratio—that is, the drag coefficient normalized by the drag coefficient of the same truck in isolation. For each of the lead and trail vehicles, two sets of data are given. For the lead vehicle, the red and blue circles represent, respectively, the drag ratio computed from the raw drag values and from the drag values corrected for blockage. The raw and corrected drag coefficient values in isolation are labeled on the plot. The drag ratio is relatively insensitive to the use of either the raw or corrected drag values, as one would anticipate. Indeed for the lead vehicle, there is no discernable difference between the two. For the trail vehicle, there is a small difference, and both curves are plotted—red for use of uncorrected data, blue for use of blockage-corrected data. The reason for the difference in this case is that the trail vehicle has a slightly greater blockage correction in tandem than it does in isolation. Our best estimate for the drag coefficient ratio of the trail vehicle would be a curve midway between the two curves presented.

The results presented in Figure 16 are qualitatively similar to the earlier single truck observations with cab-trailer gap, as for example in Figure 13(a). The rear truck (or trailer in the

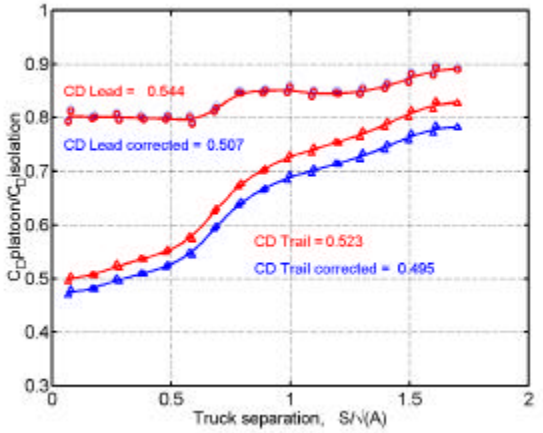

Figure 16 Dirty lead truck with dirty trail truck.

case of cab-trailer with gap) is effectively shielded for all separations tested. At short spacings—say less than 0.5—the rear truck drag decrease is of the order of 50 percent. These spacings would be difficult to realize in practice. For a full-scale truck, the square root of the cross-sectional area is about 3 meters, and a nondimensional value of 0.5 thus becomes about 1.5 meters. Beginning at 0.5, there is a steep rise in the drag of the trail vehicle to a value of approximately 70 percent of the isolation value at a distance of about 1.0, and then a continued, but more gradual, rise. All of the trail truck drag curves display this same general shape, although the magnitude of the drag savings may be different for trucks having different isolation drag values. The initial gradual rise for short spacing is due to the existence of a recirculating, cavity-like flow structure within the space between the trucks. The cavity-like flow structure consists of a relatively stable toroidal vortex (think of it as a vortex donut such as a smoke ring) occupying the space between the two trucks. The rapid rise in trail truck drag between a spacing of 0.5 and 1.0 is a result of the disappearance of this stable structure. The flow within the cavity becomes highly unsteady, and the toroidal vortex occupies the cavity for shorter periods of time. Beyond about 1.0, the flow has transitioned to a vortex-shedding wake structure that is characteristic of the flow behind all isolated bluff bodies. (These topological feature changes are known to us from our detailed studies of the flow-field within the cavity.)

Figures 17 and 18 show the relatively slight effect of increasing the drag coefficient of either the lead or the trail vehicle by incorporating a mismatched cab. Again, both trucks exhibit a reduction in drag, but the trail vehicle reduction is considerably larger. On the basis of these three figures, we conclude that if a truck operator wished to reduce drag travelling in tandem formation would do so, and the best strategy would be to follow another truck (although leading would still reduce drag).

Figure 19 displays the result for two clean trucks. Note the drag coefficients (in isolation) for the clean trucks are relatively low—probably smaller than would be realistic for any truck on the road today. Nevertheless, this case is useful as a limit. (No blockage correction is available for

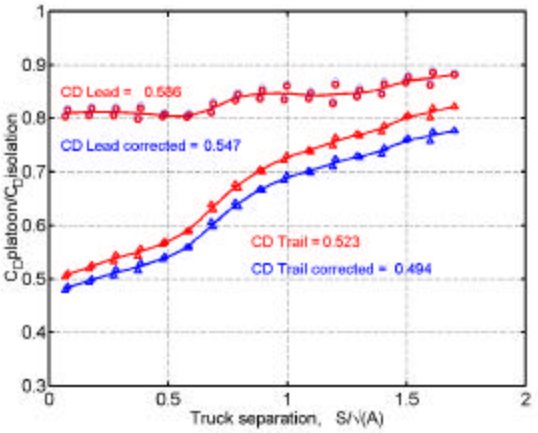

Figure 17 Dirty lead truck with mismatch followed by dirty trail truck.

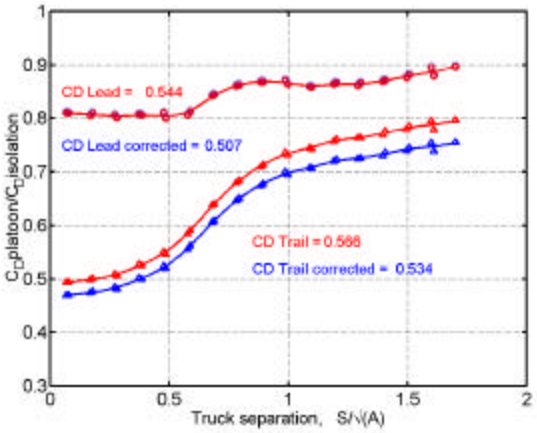

Figure 18 Dirty lead truck followed by dirty trail truck with mismatch.

this case.) The results for the clean trailer seem almost counter-intuitive, since here it is the lead vehicle that achieves the most benefit from tandem operation. The reason is as follows. For this relatively clean aerodynamic shape, most of the drag results from the relatively low pressure existing over the bluff base of the vehicle. The presence of the trail vehicle at close spacing increases the base pressure on the lead vehicle and thereby significantly reduces drag.

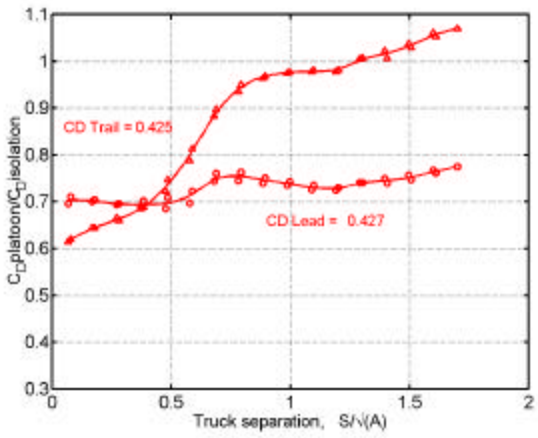

Figure 19 Clean lead truck with clean trail truck.

The aerodynamically clean trail vehicle experiences an increase in pressure over its frontal surfaces, but almost no effect on the base (far removed). The drag of the trail vehicle is thus higher—relative to its isolation value—than a less aerodynamically clean configuration.

When Dirty and Clean vehicles are mixed, as demonstrated in Figures 20 and 21, the results depend upon which vehicle leads. Clean lead-Dirty trail is greatly superior to the opposite arrangement. By leading, the aerodynamically clean vehicle gains an additional ten percent of its drag-in-isolation value at all spacings tested. Again, this is because the presence of the Dirty trail vehicle imposes a base pressure increase on the lead vehicle that is even larger than would be produced by a cleaner trail vehicle. Conversely, having the Clean vehicle to the rear diminishes the effect on the base of the Dirty lead vehicle. Since the base pressure contribution is a smaller fraction of the total drag for the Dirty vehicle, the effect of the presence of the Clean trail rapidly diminishes with increasing separation.

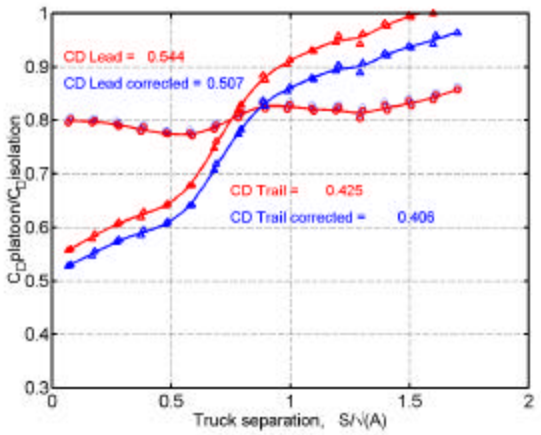

Figure 20 Dirty lead truck with clean trail truck.

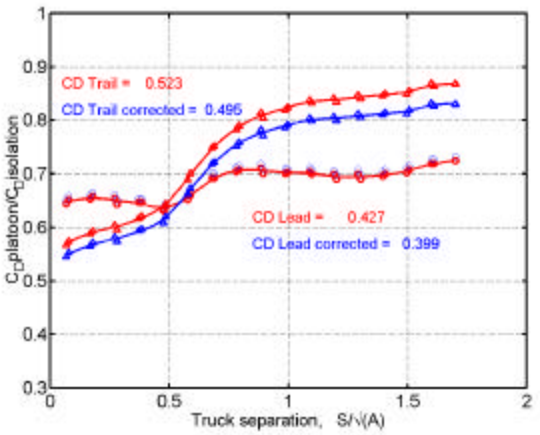

Figure 21 Clean lead truck with dirty trail truck.

An interesting composite plot can be made for the drag of the two trucks taken together, relative to the sum of their isolation drag values. The various combinations are shown quantified in Figure 22. Imagine yourself to be a fleet owner having a fleet containing aerodynamically clean

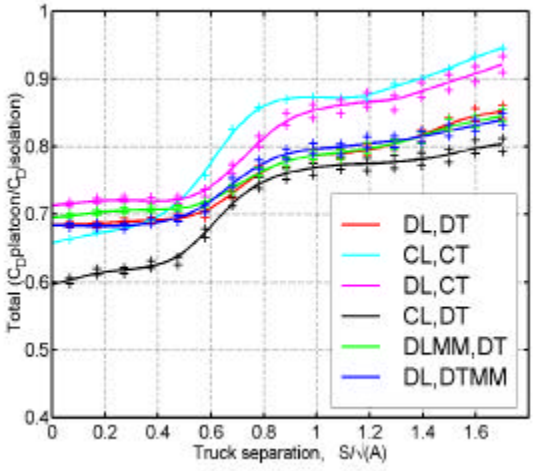

Figure 22 Total drag ratio for various platoon configurations.

and aerodynamically dirty trucks. How should they be arranged in tandem travel to minimize the total drag? This might be termed the corporate strategy. The poorest configurations to minimize total drag are the two configurations having the Clean trail. The best configuration—judged by lowest total drag—is the configuration Clean lead-Dirty trail.

Fuel Consumption for Two Trucks in Tandem

As a final and most important point, let us discuss how these results may be used to estimate the fuel consumption savings to result from tandem travel. On a level roadway, fuel is consumed to overcome aerodynamic drag and rolling resistance, and to provide a small power contribution for auxiliary devices such as alternators and air-conditioners. (This fuel expenditure accounts also for frictional losses within the engine itself—overhead as it were.) If the roadway is inclined upward, or if the vehicle is accelerating, additional fuel must be expended. These

fuel expenditures increase the kinetic and potential energies of the vehicles, and—in principle—could be recovered by judicious driving. Fuel expended to overcome aerodynamic drag and rolling resistance cannot be recovered—even in principle. Aerodynamic drag is the greater of the two at highway speeds.

Following Sovran & Bohm (1981), and Sovran (1983), one may relate the savings in fuel consumption to the savings in drag. The relationship given in Sovran & Bohm is

$$\Delta(\text{fuel consumed})/(\text{fuel consumed in isolation}) = \eta(C_{Diso}-C_{Dandem})/C_{Diso}$$

Thus the (percentage) decrease in fuel consumption is linearly related to the (percentage) decrease in drag. The sensitivity coefficient, η, depends upon the various vehicle parameters and upon the particular driving cycle chosen. For example, for an automobile following the specific EPA Highway Driving Cycle (Sovran 1983), the expression is,

$$\eta = 0.89/(1 + (0.031r_o + .000126)M/C_DA) \qquad (1)$$

where r_o is the rolling resistance coefficient, M is the vehicle mass in Kg, A is the cross-sectional area in m^2, and C_D is the drag coefficient in isolation. The EPA Driving Cycle does involve acceleration and braking. A simpler model is one for steady speed on a level roadway (Bonnet & Fritz 2000),

$$\eta = 1/(1+ 2r_oW/(\rho V^2AC_D)) \qquad (2)$$

with W the vehicle weight, ρ the air density, V the vehicle speed, and r_o, A and C_D defined as above (all quantities in consistent dimensional units). Typical values of η lie in the range η=0.6 for a fully loaded truck traveling at 70 MPH (31 m/s) and having a drag coefficient in isolation of C_D=0.6, to η=0.8 for the same truck empty. Thus, for steady travel (no acceleration/deceleration, no braking), a 25% overall drag saving would result in a 15% -- 20% fuel saving—depending upon the truck loading. These predicted results are probably overly optimistic, since driving at constant speed on a level roadway for long intervals is rarely possible.

V Acknowledgement

The authors express thanks to the California Department of Transportation, to the PATH organization and to the Department of Energy for providing the opportunity and the financial support to complete these engineering studies. Caltrans/PATH, with management responsibility of Asfand Siddiqui, provides support for the tandem truck work. The single truck at yaw is additionally funded in part by DOE, Office of Heavy Vehicle Technology, under the direction of Dr. Sid Diamond.

VI References

Bonnet, C., Fritz, H., 2000, Fuel consumption reduction experienced by two Promote-Chauffer trucks in electronic towbar operation, *SAE Paper No*. 00FTT-73.

Cooper, K.R., 1985, The effect of front-edge rounding and rear-edge shaping on the aerodynamic drag of bluff vehicles in ground proximity, *SAE paper No*. 850288.

Cooper, K.R., (editor), 1995, Closed-test-section wind tunnel blockage corrections for road vehicles, *SAE SP*-1176.

Sovran, G., Bohn, M., 1981, Formulae for the tractive-energy requirements of vehicles driving the EPA schedules, *SAE Paper No*. 810184.

Sovran, G., 1983, Tractive-energy-based formulae for the impact of aerodynamics on fuel economy over the EPA Driving Schedules, *SAE Paper No.* 830304.